Applied Catalysis B: Environmental 99 (2010) 191–197

Contents lists available at ScienceDirect

Applied Catalysis B: Environmental

journal homepage: www.elsevier.com/locate/apcatb

Visible-light photocatalytic activity of gold nanoparticles supported on template-synthesized mesoporous titania for the decontamination of the chemical warfare agent Soman

Mercedes Alvaro[a], Bogdan Cojocaru[b], Adel A. Ismail[c], Nicoleta Petrea[d], Belen Ferrer[a], Farid A. Harraz[c], Vasile I. Parvulescu[b,*], Hermenegildo Garcia[a,**]

[a] Instituto Universitario de Tecnología Química CSIC-UPV and Department of Chemistry, Universidad Politécnica de Valencia, Av. De los Naranjos s/n, 46022 Valencia, Spain
[b] Department of Chemical Technology and Catalysis, Bd. Regina Elisabeta 4-12, Bucharest 030016, Romania
[c] Advanced Materials Technology Department, Central Metallurgical Research and Development Institute (CMRDI), P.O. Box 87, Helwan, Cairo 11421, Egypt
[d] Chemical Centre of Defence NBC and Ecology Sos. Oltenitei 225, Bucharest 041309, Romania

ARTICLE INFO

Article history:
Received 3 April 2010
Received in revised form 5 June 2010
Accepted 9 June 2010
Available online 15 June 2010

Keywords:
Photocatalysis
Visible light
Chemical warfare agents
Soman
Mesoporous titania

ABSTRACT

Mesoporous titania containing gold nanoparticles has been found to be an efficient photocatalyst for the visible-light decontamination of Soman. This contrasts with the complete lack of visible-light activity of analogous mesoporous titania sample without containing Au and is attributed to light absorption by the gold nanoparticles surface plasmon band. The possibility that Soman degradation occurs by light-induced heating is unlikely since no variation of the temperature is observed in the irradiation.

The solid photocatalysts have been prepared in a single step in which incorporation of gold and formation of titania occur in the same sol–gel process. It was observed that the molar proportion of Pluronic added to the synthesis sol as template to produce mesoporosity in the material plays an important role controlling the textural properties, surface area and pore diameter, intensity of the surface plasmon band and gold loading of the solid photocatalysts.

The visible-light photocatalytic activity of mesoporous titania containing gold nanoparticles towards deadly Soman is remarkable and it constitutes an environmentally friendly system operating under ambient light at the green atmosphere without the need of corrosive or toxic chemicals.

1. Introduction

While TiO_2 is the most widely used photocatalyst that exhibits an almost universal activity for the degradation of organic compounds, there is still a continuous need to prepare new modified titania materials with higher photoefficiency [1–8]. Particularly, one of the major limitations in the use of TiO_2 is its lack of photochemical activity under visible-light illumination [1]. Considering that solar light has only about 3–5% of UV light and that most of the solar energy corresponds to the visible and near IR regions, the photo-action spectrum of anatase TiO_2 is clearly unsatisfactory for ambient light or sunlight irradiation because TiO_2 will only respond to a very narrow range of wavelength [1,2,7,9–12]. Besides the limitation of TiO_2 with respect to the excitation wavelength, also electron/hole annihilation is an unfavourable pathway that decreases significantly the photocatalytic efficiency of this material.

To increase the photocatalytic efficiency of pure TiO_2 several strategies have been developed, the most widely used being doping with metallic and non-metallic elements [13–19]. One recent strategy that derives in part from heterogeneous catalysis is the use of titania-supported gold nanoparticles (Au/TiO_2) as photocatalyst [20–27]. Since the pioneering work of Haruta showing the unique catalytic activity of Au/TiO_2 for the selective low-temperature CO oxidation [28,29], the number of reports describing the use of Au/TiO_2 as heterogeneous catalyst for thermal reactions has grown considerably [30–32]. These works in heterogeneous catalysis have shown how to prepare in a reliable and reproducible way Au/TiO_2 samples (around 1.5 wt%) constituted by gold nanoparticles with a narrow size distribution (about 5 nm) strongly fixed on the surface of TiO_2 nanoparticles (about 30 nm) mainly in the anatase phase. Although low-temperature CO oxidation is far from photocatalytic reactions, it should be noted that Au/TiO_2 typically used in heterogeneous catalysis should be in principle also very promising as photocatalyst because having stable noble metal nanoparticles

* Corresponding author.
** Corresponding author. Tel.: +34 963877807; fax: +34 963877809.
E-mail addresses: vasile.parvulescu@g.unibuc.ro (V.I. Parvulescu), hgarcia@qim.upv.es (H. Garcia).

0926-3373/$ – see front matter © 2010 Elsevier B.V. All rights reserved.
doi:10.1016/j.apcatb.2010.06.019

strongly anchored onto TiO_2 surface as an independent phase no photo-corrosion, typically observed when doping, should occur. Thus, our hypothesis is that having reliable procedures to develop TiO_2 supported gold nanoparticles these materials can also be useful as photocatalysts.

One of the most remarkably properties of gold nanoparticles is the presence of a visible band around 560 nm denoted as surface plasmon band (SPB) that arises from the collective excitation of electrons confined in the metal nanoparticles [33–36]. In principle, the use visible light to excite this SPB of gold nanoparticles with the injection of electrons on the TiO_2 conduction band could be possible. In a certain way, the photocatalytic mechanism of Au/TiO_2 could resemble that of the general dye sensitization mechanism of TiO_2 [37,38]. In previous works using UV light to produce excitation of the TiO_2 semiconductor it has been proposed that electrons in the conduction band of the semiconductor migrate to gold nanoparticles acting as electron reservoir. In the present case, we are going to use UV filtered visible light that cannot produce excitation of TiO_2. Controls using analogous samples without gold will show no photocatalytic activity at all, thus proving that not direct excitation of TiO_2 occurs. However, considering the low reduction energy of the conduction TiO_2 band [39] and that metal nanoparticles of small size can behave as semiconductors [40–42], photoinduced electron injection from gold nanoparticles to TiO_2 promoted by visible light could be a viable process.

There are some precedents reporting the photoactivity of gold nanoparticles as sol on supported TiO_2 [40,43–45]. Most of the previous studies using this type of Au/TiO_2 have nevertheless used UV light and have proposed direct excitation of TiO_2 in the semiconductor band-gap, the role of Au nanoparticles being as electron traps and catalytic sites. The number of photocatalytic studies in which visible-light activity of Au/TiO_2 have been tested is still relatively small and has led to contradictory results [25,46]. Thus, for the photo-oxidation of cyclohexane Carneiro et al. have reported that the deposition of gold even decreases the photocatalytic activity of TiO_2 because in this process surface hydroxy groups of titania are needed to generate hydroxy radicals and the formation of hydroxyl groups is impeded by coverage of the titania surface hydroxyl groups by gold [47]. Thus, the data currently available do not allow anticipating the photocatalytic activity of Au/TiO_2, particularly under visible-light irradiation.

In the present manuscript, we describe the visible-light photocatalytic activity for special Au/TiO_2 samples that have been prepared in a single-step process in which gold nanoparticles and TiO_2 have been formed simultaneously by sol–gel. The most relevant synthetic characteristic is the use of a triblock copolymer as template to produce mesoporosity in the material. For this reason the samples under study have been termed as $Au/mpTiO_2$, wherein "*mp*" alludes to the mesoporosity introduced by the amphiphilic copolymer used in the synthesis. Photocatalysis, being an interfacial phenomenon, is benefited from materials with surface area as large as possible to promote the interaction of adsorbates with electrons/holes on the particle surface. Typical surface areas of commercial Au/TiO_2 are about 50 m^2/g and there is much interest in preparing materials with larger surface area. Also, commercial Au/TiO_2 samples are prepared by the deposition/precipitation method that consists of formation of gold nanoparticles on preformed TiO_2 through a two-step (surface $AuCl_4^-$ adsorption/nanoparticle formation) process. It would be much more desirable to obtain these materials in a single step in which gold and titania particles are formed simultaneously.

We have applied these materials to a challenging problem of large societal concern, as is the degradation of deadly toxic chemical Soman. Organophosphorous compounds found wide used as pesticides and some of them such as Soman are also chemical weapons [48–51]. Development of an efficient visible-light photocatalyst can be useful as counter measure to deal with emergency situations caused by chemical spill over [52]. We will show that $Au/mpTiO_2$ (Au loading from 0.5 to 0.7 wt%) operates under visible-light irradiation producing complete degradation of Soman in reasonable exposition times.

2. Experimental

2.1. Titania and Au/titania syntheses

The triblock copolymer surfactant $EO_{106}–PO_{70}–EO_{106}$ (commercially denoted as Pluronic F127, $EO = –CH_2CH_2O–$, $PO = –CH_2(CH_3)CHO–$) was obtained from Sigma. Titanium tetraisopropoxide, $Ti[OCH(CH_3)_2]_4$ (TTIP), methanol and $HAuCl_4$ were purchased from Aldrich and all chemicals were used as received. Mesoporous titania, $mpTiO_2$, and nanocrystalline gold/mesoporous titania, $Au/mpTiO_2$, were synthesized through a one-step, sol–gel process in the presence of a F127 triblock copolymer as structure directing agent. To homogenously embed gold nanoparticles within the titania framework, a multicomponent assembly approach was utilized, where surfactant, titania, and gold building clusters were cooperatively assembled in a one-step process. Four samples in where the amount of F127 surfactant was increased were prepared. The preparation procedure for $mpTiO_2$ and $Au/mpTiO_2$ was as follows:

Firstly, the required amount of the triblock copolymer F127 was dissolved in 11 g of methanol by stirring for 30 min. Then, a solution of 9.84 g of TTIP in 1.44 ml HCl (37%) was added under vigorous stirring for 10 min, followed by dropwise addition of an aqueous solution (0.64 ml) containing $HAuCl_4$ (0.04 g/ml), corresponding to a theoretical gold loading in the material of 0.5 wt%. To minimize possible variables, except the amount of F127, the molar ratio of the other reagents in the starting solution was fixed at $TiO_2/F127/HCl/H_2O/CH_3OH = 1:X:1:4:10$ four different samples were prepared varying the molar amount of F127 (X) from 0.005, 0.0075, 0.01 and 0.0125. For each of the four samples, the sols were gelled at 40 °C in air for 30 min.

The obtained Au/TiO_2 gels were dried under ambient conditions to induce crosslinking and oligomerization of the TiO_2 of the sol/gel precursor. The gelation time was significantly reduced, from 7 days to 30 min as a result of addition TTIP instead of $TiCl_4$ [53]. In order to reduce $HAuCl_4$ forming metallic Au nanoparticles, the gels were treated with deep UV irradiation in air ($\lambda = 254$ nm) for 2 days. This treatment should produce some degradation of F127 acting as sacrificial electron donor of Au photo-deposition. The gel samples were calcined at 500 °C for 4 h with a heating rate of 2 °C/min and cooling rate of 2 °C/h in air to remove completely the surfactant, promote the crystallization of TiO_2 into anatase phase and the introduction of interparticle mesopores. The complete removal of the surfactant was confirmed by combustion chemical analysis that shows that the samples are carbon free.

2.2. Materials characterization

X-ray diffraction (XRD) data were acquired on a Brucker AXS D4 Endeavour X diffractometer using Cu $K\alpha_{1/2}$, $\lambda\alpha_1 = 154.060$ pm, $\lambda\alpha_2 = 154.439$ radiation. Typically, the data were collected from 20° to 80° (2θ) with a resolution of 0.02° and a count time of 4 s at each point. The nitrogen adsorption and desorption isotherms at 77 K were measured using a Quantachrome Autosorb 3B after the samples were vacuum-dried at 200 °C overnight. The sorption data were analyzed using the Barrett–Joyner–Halenda (BJH) model with Halsey equation [54]. The thermogravimetric analysis of the $Au/mpTiO_2$ gels before and after UV treatment was carried out at a heating rate 10 °C/min from 20 to 1000 °C in flowing air

(Setaram, Setsys Evolution-1750). FTIR spectra were recorded with a BRUKER FRA 106 spectrometer using the standard KBr pellet method. TEM was conducted at 200 kV with a JEOL JEM-2100F-UHR field-emission instrument equipped with a Gatan GIF 2001 energy filter and a 1k-CCD camera in order to obtain EEL spectra. SEM images were obtained on a JEOL JSM-6700F field-emission instrument using a secondary electron detector (SE) at an accelerating voltage of 2 kV. The band-gap energy of the catalysts was determined using diffuse reflectance spectroscopy (DRS). The reflectance spectra of the samples over a range of 200–700 nm were recorded by a Varian Cary 100 Scan UV–vis system equipped with a Labsphere diffuse reflectance accessory. The spectrophotometer was equipped with an integrating sphere, and $BaSO_4$ was used as the standard for total reflection [55]. A given amount of $mpTiO_2$ and $Au/mpTiO_2$ powder was uniformly pressed in the tablet and placed in the sample holder on integrated sphere for the reflectance measurements. The reflectance data was converted to the absorption coefficient $F(R)$ values according to the Kubelka–Munk equation [56–57]. The modified Kubelka–Munk function was determined using the Eq. (1) as follows:

$$F(R) = \left(\frac{(1-R)^2}{2R} \times h\upsilon \right)^{1/2} \quad (1)$$

where R is the proportion reflected, h is Planck's constant, and υ is the frequency of light. $F(R)$ plots versus energy were used to determine band-gap energy by calculating a linear fit for the linear portion of the absorption transition using least squares regression and extrapolating to zero at the corresponding photon energy. The band-gap energies of photocatalysts were calculated according to the band-gap equation (EG) = hc/λ, where EG is the band-gap energy (eV), c the light velocity (m/s), estimated error ± 1 m/s and the wavelength (nm) experimental error ± 1

2.3. Photodecomposition of pinacolyl methylphosphonofluoridate (Soman)

The photocatalytic activity of $mpTiO_2$ and $Au/mpTiO_2$ for the decomposition of Soman was determined by exposing to visible light the solid photocatalysts contaminated with a 0.77% Soman solution. Soman was adsorbed onto the photocatalysts by evaporation of methylene chloride solutions containing the required Soman amount. The experiments were carried out in a closed quartz tube flushed with a constant air flow (50 $cm^3\ min^{-1}$). As irradiation source a 200 W Ne lamp (F74-765, Tungsram, Hungary) with a wavelength emission range from 420 nm to IR and a maximum emission at 600 nm and light intensity of 4300 Lx (measured with an 840006 Speer Scientific luxmeter) was used. The emission spectrum of this lamp having a limit at 420 nm makes no necessary to use cut-off filters to avoid UV light. The Soman samples for the tests were supplied and manipulated by N.B.C. Defence and Ecology Scientific Research Centre of Romanian Ministry of Defence. It should be reminded that the production and use of these chemical warfare agents is strictly regulated under an international convention for the prohibition of this type of weapons [50]. The evolution of the reaction was followed by taking one vat at the required reaction time, extracting the photocatalyst with dichloromethane, concentrating the resulting extracts and analyzing after derivatization the solution by GC/MS equipment Thermo Electron Trace GC – DSQ. Derivatization by *N*,*N*-bis-(trimethylsilyl/trifluoroacetamide) containing 10% of chlorotrimethylsilane was performed by adding a drop of this reagent to the extraction residue and heating at 60 °C for 30 min. The initial sample, one blank control unexposed to visible light, and the irradiated samples were subjected to identical extraction procedure with 500 μl solvent mixture. Before GC/MS injection, the reaction mixture was derivatized by treatment with *N*,*N*-bis(trimethylsilyl)trifluoracetamide in methylene dichloride to produce volatile trimethylsilyl derivatives of the degradation by-products. Besides analysing the products present on the solid photocatalyst, samples of the gas phase inside the reactor were taken at regular intervals with a gas-tight syringe and analyzed using a GC/MS. The decontamination rate was calculated as the percentage of compound consumed from the initial quantity. Analytical data from the control unexposed to visible light shows that no dark degradation or hydrolysis of Soman occurs.

The decontamination degree was calculated using the data provided from the spiking solution (100 μl Soman solution 0.77% in 500 μl extraction solvent). The purity of the original toxic chemical Soman is 98%, as determined by the GC/MS analysis.

3. Results and discussion

As commented in the introduction, the main purpose of our work is to show visible-light, photocatalytic activity of mesoporous titania containing gold nanoparticles ($Au/mpTiO_2$). The gold loading of our samples has been set to be in the range typically used in heterogeneous catalysis that is considerably smaller than those of previous samples whose photophysics has been studied by laser flash techniques [40,41,44]. We also have prepared the samples in a single step in which incorporation of gold and formation of titania occur in the same synthesis process. Therefore, compared to reported preparation procedures, the obtainment of our $Au/mpTiO_2$ is very simple since our method is not stepwise synthesis of mesoporous TiO_2 followed by deposition of gold nanoparticles. A third feature of our synthesis is the use of triblock copolymers as surfactant to create mesoporosity in the material. Large mesoporosity and surface area are always beneficial for the photocatalytic activity. UV irradiation of the as synthesised $Au/mpTiO_2$ produces photocatalytic formation of Au nanoparticles and calcination promotes the crystallization of TiO_2 as anatase and leads to the decomposition of F127 template.

In the present study we have prepared four samples starting from the same sol composition, except that the molar amount of F127 surfactant that has been varied. Since in the synthesis the surfactant copolymer acts as structuring directing agent creating mesoporosity and spatial structuring as well as ligand of gold, variation of the surfactant concentration in the synthesis sol must lead to changes in the gold loading, surface area, mesoporosity and, as result, on the photocatalytic activity of the resulting $Au/mpTiO_2$ materials. Herein, the concentration of surfactant has been varied from 0 to the common 0.0125 molar fraction typically used in the synthesis of mesoporous silicas [58–60]. Thus, four $Au/mpTiO_2$ materials have been prepared and tested for their photocatalytic activity.

3.1. Structural and textural investigation

Powder XRD provides information about the crystal phase, composition, and particle size of materials. Fig. 1 shows the diffraction pattern after calcination of pure $mpTiO_2$ sample with a $F127/TiO_2$ mole ratio of 0.005 showing the typical peaks for the anatase phase that corresponds to (1 0 1), (0 0 4), (2 0 0) and (2 1 1) lattice planes (powder diffraction file no. 86-1157, ICCD). For the series of the four $Au/mpTiO_2$ (0.5 Au wt%) photocatalysts prepared at various F127 molar amounts, no crystalline phase attributable to gold was observed for the calcined samples. This indicates that either the Au content is below the detection limit or that the gold is highly dispersed in the TiO_2 network. The primary TiO_2 crystal size evaluated from the Scherrer equation using the full width at half maximum (FWHM) values of the diffraction peaks is 5 nm.

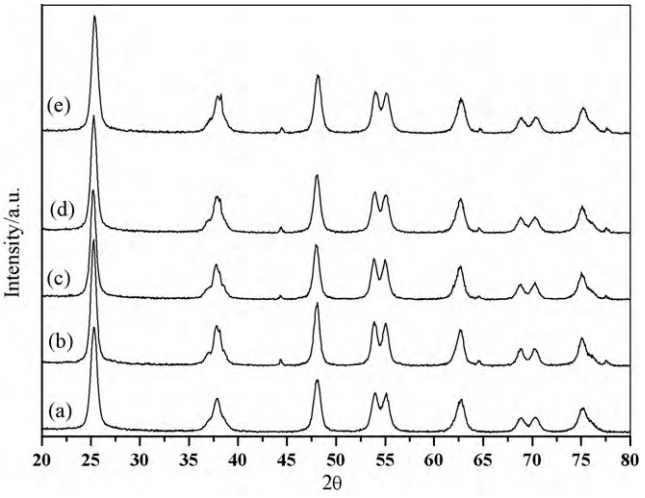

Fig. 1. Powder XRD patterns for pure $mpTiO_2$ at $F127/TiO_2$ mole ratio 0.005 (a) and $Au/mpTiO_2$ nanocrystals at $F127/TiO_2$ mole ratios 0.005 (b), 0.0075 (c), 0.01 (d), and 0.0125 (e), respectively, after calcination at 500 °C for 4 h.

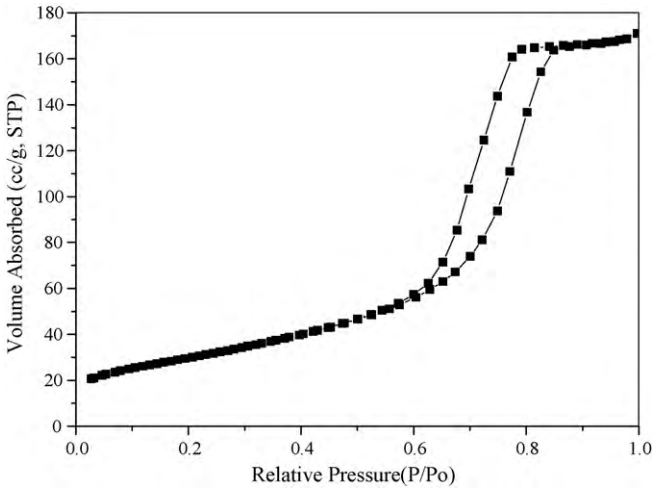

Fig. 3. Nitrogen adsorption–desorption isotherms for mesoporous $mpTiO_2$ after calcination at 500 °C for 4 h.

TEM images of nanocrystalline $Au/mpTiO_2$ solids are presented in Fig. 2. An overview image at low magnification illustrates that the product is almost exclusively composed of discrete titania nanoparticles without the formation of large agglomerates. Higher expansions show that the TiO_2 particles are quite uniform in size and shape (Fig. 2b). TEM data are in line with the XRD results showing an average particle size for the TiO_2 crystallites of ~5 nm. HRTEM image (Fig. 2c) and selective area electron diffraction (SAED, inset Fig. 2c) shows well resolved diffraction patterns indicative of a highly crystalline anatase framework with the lattice (1 0 1) fringe of 0.352 nm. TEM image of the $Au/mpTiO_2$ photocatalyst recorded under dark field conditions shows the presence of homogeneously dispersed gold nanoparticles adsorbed on the TiO_2 support.

The uniform nanocrystalline particle size distribution of TiO_2 (5 nm) should be correlated with the preparation procedure based on the use of the Pluronic F127 surfactant in methanol [53]. Concerning the crystal phase, it has been established that the crystal phase stability is particle size dependent, and for particle with diameters <14 nm, anatase is more stable than rutile phase [61].

One important issue related to the use of surfactant in the synthesis and revealed by PXRD and TEM is that although the presence of the F127 copolymer in the $Au/mpTiO_2$ materials (even in the largest mole fraction ratio) introduces mesoporosity, there is no periodic structuring in the material and the mesopores lack of spatial ordering that has been found for mesoporous silicas synthesized under similar conditions. In this regard it is convenient to comment that periodicity and regularity is not a prerequisite for high photocatalytic activity that could be achieved even if the mesopores are not spatially ordered.

Concerning mesoporosity, Fig. 3 shows typical nitrogen sorption isotherms for the synthesized $mpTiO_2$. In the case of $Au/mpTiO_2$ samples prepared at various F127 molar amounts and submitted to calcination at 500 °C for 4 h, similar nitrogen sorption profiles were observed. They are characterized by large hysteresis loops that resemble typical H2-type N_2 adsorption/desorption isotherms. Such hysteresis is assumed to be related to the capillary condensation associated with large pore channels. Table 1 summarizes the

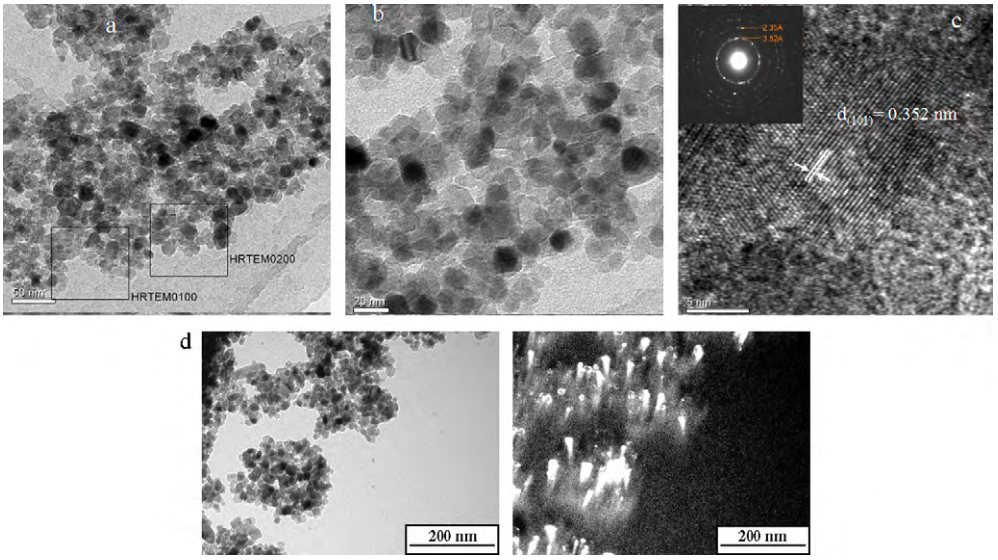

Fig. 2. Representative TEM micrographs of a sample calcined at 500 °C for 4 h. (a) The overview proves an homogeneous particle size distribution of titania nanoparticles with an average diameter of about 5 nm; (b) higher magnification demonstrates that the particles are not agglomerated and quite uniform in size and shape. HRTEM image titania nanoparticles (c) and selective area electron diffraction (SAED, inset c); (d) TEM images of $Au/mpTiO_2$-2 (F127/TTIP 0.0075) recorded in bright field (left) and dark field (right), demonstrating the presence of gold in the solid.

Table 1
Physicochemical properties of pure $mpTiO_2$ and of $Au/mpTiO_2$ nanoparticles prepared with different F127/TTIP molar ratios.

Acronym	F127/TiO_2 mole ratio	Surface area (m^2/g) error $\pm 3\ m^2/g$	Pore size (nm) error ± 0.2 nm	Au content (weight %)
$mpTiO_2$	0.010	113	6.0	–
$Au/mpTiO_2$-1	0.005	90	7.1	0.70
$Au/mpTiO_2$-2	0.0075	81	6.5	0.37
$Au/mpTiO_2$-3	0.010	81	5.7	0.45
$Au/mpTiO_2$-4	0.0125	110	6.5	0.43
CommercialAu/TiO_2[a]	–	38	Non-porous	1.5

[a] Commercial sample available from the World Gold Council as reference catalyst.

main porosity data obtained from the isothermal N_2 sorption measurements. As it can be seen there, Barrett–Joyner–Halenda (BJH) analyses comparing the $mpTiO_2$ and the $Au/mpTiO_2$ prepared at the same F127 molar concentration shows that the presence of gold nanoparticles reduces the surface area and average pore size (compare entries 1 and 4 of Table 1). Importantly, as it was anticipated the data from Table 1 also proves experimentally that the proportion of F127 controls the surface area, porosity and the final Au content of the resulting Au/TiO_2 samples. This can be easily rationalized considering the main function of the F127 surfactant as mesoporosity promoter and its role complexing $AuCl_4^-$ and generating Au nanoparticles in the photo-reduction process.

However, as it can be seen in the Table 1, there is not a clear correlation among the amount of template added in the sol and the three main textural and analytical data. Thus, the final Au content does not control the surface area and mesoporosity that appear to be the result of a combination of the templating effect of F127 and the Au loading. Also, the total surface area and average mesopore diameter are uncorrelated as consequence of the differences in Au loading among the various samples. In any case, the data of Table 1 show that compared to commercial unstructured Au/TiO_2, the use of F127 template produces samples with over threefold larger surface area, with relatively narrow mesopores and with lower Au content.

Fig. 4 presents the FTIR spectra for as-made $Au/mpTiO_2$-3 (F127 molar amount 0.010) sample and after UV treated for 2 days and final calcination. It should be noted that although UV treatment does not effect significant degradation of the template, this was achieved in the calcination step as demonstrated by combustion chemical analysis. The other samples exhibit very similar FTIR spectra and behavior. The as-synthesised $Au/mpTiO_2$-3 (F127 0.010) exhibits a band at 2875 cm^{-1} accompanied by the peaks 1460 and 1378 cm^{-1} that can be attributed to stretching and bending modes characteristic of CH_2 and CH_3 groups present on the template. Also the 1115 cm^{-1} should correspond to the C–O stretching vibration band of the F127 polymer. The broad absorbance in the range from 3000 to 3500 cm^{-1} and the absorbance band around 1643 cm^{-1} are attributed to the vibrations of the surface-adsorbed H_2O and Ti--OH bonds respectively [62]. The bands at 1242 and 1297 cm^{-1} could be attributed to the TiO_2 network in contact with template [63]. After baseline correction and normalization of the 1115 cm^{-1} peak similar FTIR spectrum is recorded for the $Au/mpTiO_2$-3 sample after the UV treatment with negligible changes in the intensity of the bands corresponding to the F127 template. This indicates that the photo-reduction process to generate gold nanoparticles, barely effects the photocatalytic decomposition of the organic template. This is not surprising considering that the mesopores are full of polymer impeding the access of oxygen and water needed in the photocatalytic decomposition of organic substrates. The bulk removal of the organics was achieved by calcination at 500 °C for 4 h. FTIR spectrum of the calcined $Au/mpTiO_2$ shows the presence of surface hydroxyl groups. Surface hydroxyl play an important role in the photocatalytic activity of the material because the holes generated under UV light irradiation are trapped by these surface hydroxyls groups to form hydroxyl radicals, suppressing in this way electron-hole recombination, hence increasing the photocatalytic efficiency.

Fig. 5 shows the DR–UV–vis spectra for the $Au/mpTiO_2$ series compared with pure mesoporous $mpTiO_2$. As expected, the presence of gold nanoparticles introduces in the optical spectra an additional absorption band in the visible region at around 550 nm due to gold surface plasmon band. We notice, however, that the surface plasmon band is very broad expanding up to 900 nm indicating a heterogeneity in sizes and shapes of gold nanoparticles. This broad absorption band in the visible region can be favourable from the photocatalytic point of view since ensures absorption in a wide wavelength region and should be responsible for visible-light

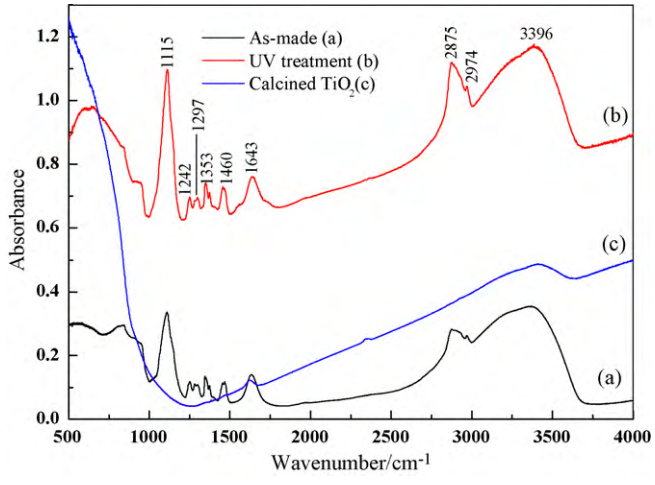

Fig. 4. FTIR spectra for $Au/mpTiO_2$ (F127/TTIP 0.010) as made (a), after UV illuminated for 2 days (b) and after calcination (c).

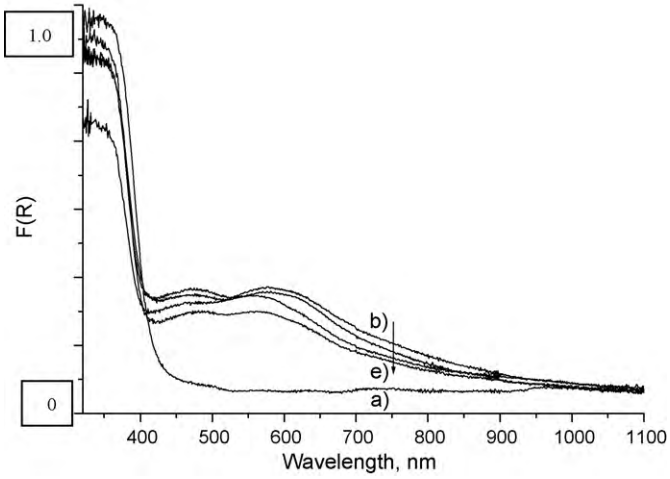

Fig. 5. Diffuse reflectance UV–vis spectra (plotted as the Kubelka-Munk function of the reflectance, R) for $mpTiO_2$ (a) and the four $Au/mpTiO_2$ samples at F127 molar ratio of 0.005 (b), 0.0075 (c) 0.010 (d) and 0.0125 (e).

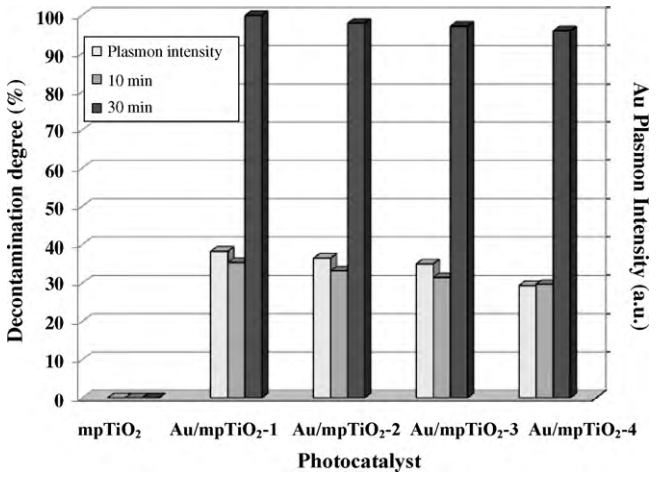

Fig. 6. Percentage of Soman decontamination after 10 and 30 min visible-light irradiation and intensity of the Au surface plasmon band for the series of Au/mpTiO$_2$ photocatalysts.

absorption of Au/mpTiO$_2$ solids that is the origin of the photocatalytic activity under these conditions. Absorption corresponding to the interband transition of gold (5d → 6sp) is also visible around 450 nm [64]. A variation in the intensity of these absorption bands is observed in the series depending on the preparation conditions. This can be correlated with the gold loading, the local dielectric constant experienced by the nanoparticles in accordance with the previous data showing that the position and intensity of the surface plasmon band of gold nanoparticles strongly depends on their size, shape and charge density [64,65].

The optical band-gap of the investigated catalysts was calculated based on the UV–vis measurements extrapolating to the crossing wavelength the best fit of the linear part of the absorption band. According to these measurements mpTiO$_2$ showed a band-gap of 2.97 eV. The introduction of gold led to a slight increase of the catalysts band-gap with an average value of 0.1 ± 0.02 eV irrespective of the preparation composition. This small shift could be due to a very minor extent of Au-doping of mpTiO$_2$ framework while being formed.

3.2. Decontamination of Soman with mpTiO$_2$ and Au/mpTiO$_2$ nanocomposites under visible light

The mpTiO$_2$ and Au/mpTiO$_2$ catalysts (20 mg) were spiked with 100 μl Soman 0.77% solution in methylene chloride. Control experiments were performed under the same conditions in the dark. No conversion of Soman has been observed under these conditions. The photocatalysts were exposed to visible light for times till 120 min. However, after 30 min the conversion was almost complete and the decontamination degree varied between 93% and 99.9%. Fig. 6 shows the decontamination degree after 10 and 30 min, respectively. The chromatographic analyses confirmed that the hydrolysis process of the toxic compounds in the presence of the photocatalysts starts only after ~10 min. To compare the photocatalysts performance using the decontamination degree it appears more coherent to consider it after 10 min since this shorter time corresponds better to the initial reaction rate and report better on the intrinsic photocatalytic efficiency of the Au/mpTiO$_2$ material than longer times when all the photocatalytic reactions have almost gone to completion (see Fig. 6).

As mentioned above, there were no differences among the band-gap of the Au/mpTiO$_2$ photocatalysts and the only influence of the addition of $AuCl_4^-$ in the sol to form gold nanoparticles is a slight increase in the band-gap of the Au/mpTiO$_2$ materials compared with the pure titania. On the other side, as expected in view of the general lack of response of titania to visible light, pure mpTiO$_2$ was completely inactive for the decomposition of Soman under the irradiation conditions employed here with visible light. Thus, it can be concluded that the Soman conversion is not due to direct excitation of titania in its band-gap of the catalysts.

In contrast, the photocatalytic data taken at 30 min that are presented in Fig. 6 demonstrate a linear correlation between the Soman conversion and the intensity of the surface plasmon band of gold, as this has been determined by diffuse reflectance UV–vis. 30 min was found an adequate exposure time since shorter times are subjected to larger errors due to lower conversions and longer time will level off the activity of the most active materials. Both the relative intensity of the surface plasmon band and the Soman conversion decreased when the proportion of template increase (Fig. 6). The possibility that the effect is due to some heating of the sample due to the conversion of visible light into heat seems unlike since no noticeable temperature increase was observed during irradiation of the samples.

It should be noted that the photocatalyst with higher efficiency for Soman decontamination is the one with lower template proportion and higher gold loading. Since chemical analysis confirm the complete removal of the template and the absence of carbon in the samples, the photocatalytic activity order must be due to other factors. Therefore, it can be concluded that the optimal textural properties of the photocatalyst for Soman decontamination are medium surface area, 90 m^2/g, and large pore diameter, 7.1 nm with the highest Au loading. These characteristics are reached with the lowest proportion of F127 template used.

To put into context the efficiency of Au/mpTiO$_2$ and stablish the influence of mesoporosity on the photocatalytic activity we have included in our study a P25 supported gold photocatalyst, Au/TiO$_2$, that has been earlier studied for the same reaction [66]. Performing the photocatalytic experiments under the same conditions as those used for Au/mpTiO$_2$ materials we observed that Au/TiO$_2$ is able to achieve15 and 47% at 10 and 30 min irradiation time, respectively. These Soman decontamination values achieved for commercial Au/TiO$_2$ are clearly inferior than those shown in Fig. 6 for the mesoporous materials that are more than twice more

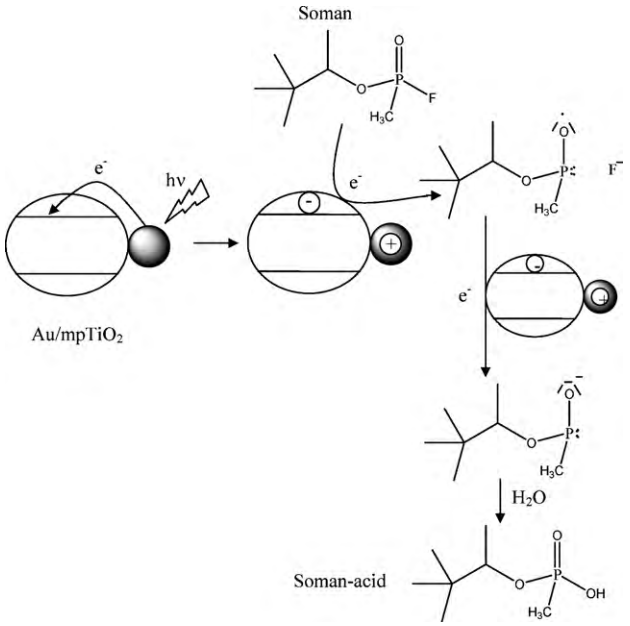

Scheme 1. Proposed mechanism for the Soman degradation by the Au/mpTiO$_2$ photocatalyst.

active than the non-porous sample, thus providing experimental evidence that mesoporosity and surface area plays a beneficial role on the degradation process.

As the Soman is photolyzed by surface hydroxyls and/or physisorbed water on the TiO_2 (*see FTIR measurements*) the major product is the so-called Soman-acid, accompanied by about 18% methyl phosphonic acid [67]. As depicted in Scheme 1, Soman-acid and methyl phosphonic acid will be most certainly in the ionized form due to the basic nature of the TiO_2 surface.

4. Conclusions

In this paper, we have been able to observe and quantify visible-light photocatalytic activity of mesoporous titania containing gold nanoparticles for Soman decontamination. This contrasts with the complete lack of activity of analogous $mpTiO_2$ sample without containing Au and is attributed to light absorption by the gold nanoparticles surface plasmon band. The occurrence of a thermal degradation is unlikely since no variation of the temperature is observed in the irradiation.

Suitable solid photocatalysts can be prepared in a single step in which incorporation of gold and formation of titania occur in the same sol–gel process. The data presented allow to conclude that the molar proportion of F 127 added to the synthesis sol as template to produce mesoporosity in the material plays an important role controlling the textural properties, surface area and pore diameter, intensity of the surface plasmon band and gold loading of the solid photocatalysts. The material exhibiting the highest photocatalytic efficiency for Soman decontamination is the one with lowest template proportion and higher gold loading. The complete conversion of Soman was achieved in only 30 min.

Considering the current interest in developing efficient decontamination methods that could be used under emergency situations caused by toxic chemicals spill over on terrorist attacks, the visible-light photocatalytic activity of $Au/mpTiO_2$-1 (F127 0.005 molar amount) towards deadly Soman is remarkable since it could constitute an environmentally friendly system operating under ambient light at the green atmosphere without the need of corrosive or toxic chemicals.

Acknowledgements

Partial financial support by Egyptian–Spanish program (PCI A/8244/07 EGIPTO) and NATO (collaboration between Romania and Spain) are gratefully acknowledged.

References

[1] M. Anpo, M. Takeuchi, Journal of Catalysis 216 (2003) 505.
[2] O. Carp, C.L. Huisman, A. Reller, Progress in Solid State Chemistry 32 (2004) 33.
[3] M.A. Fox, M.T. Dulay, Chemical Reviews 93 (1993) 341.
[4] U.I. Gaya, A.H. Abdullah, Journal of Photochemistry and Photobiology C-Photochemistry Reviews 9 (2008) 1.
[5] M.R. Hoffmann, S.T. Martin, W.Y. Choi, D.W. Bahnemann, Chemical Reviews 95 (1995) 69.
[6] A.L. Linsebigler, G.Q. Lu, J.T. Yates, Chemical Reviews 95 (1995) 735.
[7] M.I. Litter, Applied Catalysis B-Environmental 23 (1999) 89.
[8] A. Mills, S. LeHunte, Journal of Photochemistry and Photobiology A-Chemistry 108 (1997) 1.
[9] A.G. Agrios, P. Pichat, Journal of Applied Electrochemistry 35 (2005) 655.
[10] D. Chatterjee, S. Dasgupta, Journal of Photochemistry and Photobiology C-Photochemistry Reviews 6 (2005) 186.
[11] A.V. Emeline, V.N. Kuznetsov, V.K. Rybchuk, N. Serpone, International Journal of Photoenergy (2008).
[12] M. Kitano, M. Matsuoka, M. Ueshima, M. Anpo, Applied Catalysis A-General 325 (2007) 1.
[13] C. Aprile, A. Corma, H. Garcia, Physical Chemistry Chemical Physics 10 (2008) 769.
[14] X.B. Chen, Y.B. Lou, S. Dayal, X.F. Qiu, R. Krolicki, C. Burda, C.F. Zhao, J. Becker, Journal of Nanoscience and Nanotechnology 5 (2005) 1408.
[15] V.P. Indrakanti, J.D. Kubicki, H.H. Schobert, Energy and Environmental Science 2 (2009) 745.
[16] G. Liu, L.Z. Wang, C.H. Sun, X.X. Yan, X.W. Wang, Z.G. Chen, S.C. Smith, H.M. Cheng, G.Q. Lu, Chemistry of Materials 21 (2009) 1266.
[17] S. Rehman, R. Ullah, A.M. Butt, N.D. Gohar, Journal of Hazardous Materials 170 (2009) 560.
[18] N. Serpone, Journal of Physical Chemistry B 110 (2006) 24287.
[19] G.D. Sheng, J.X. Li, S.W. Wang, X.K. Wang, Progress in Chemistry 21 (2009) 2492.
[20] L. Alaerts, J. Wahlen, P.A. Jacobs, D.E. De Vos, Chemical Communications (2008) 1727.
[21] A. Dobosz, A. Sobczynski, Monatshefte Fur Chemie 132 (2001) 1037.
[22] A. Orlov, M.S. Chan, D.A. Jefferson, D. Zhou, R.J. Lynch, R.M. Lambert, Environmental Technology 27 (2006) 747.
[23] R.S. Sonawane, M.K. Dongare, Journal of Molecular Catalysis A-Chemical 243 (2006) 68.
[24] V. Iliev, D. Tomova, L. Bilyarska, G. Tyuliev, Journal of Molecular Catalysis A-Chemical 263 (2007) 32.
[25] V. Rodriguez-Gonzalez, R. Zanellac, G. del Angela, R. Gomeza, Journal of Molecular Catalysis A-Chemical 281 (2008) 93.
[26] B.K. Min, J.E. Heo, N.K. Youn, O.S. Joo, H. Lee, J.H. Kim, H.S. Kim, Catalysis Communications 10 (2009) 712.
[27] Y.M. Wu, H.B. Liti, J.L. Zhang, F. Chen, Journal of Physical Chemistry C 113 (2009) 14689.
[28] D. Cunningham, S. Tsubota, N. Kamijo, M. Haruta, Research on Chemical Intermediates 19 (1993) 1.
[29] M. Haruta, Catalysis Today 36 (1997) 153.
[30] A. Corma, H. Garcia, Chemical Society Reviews 37 (2008) 2096.
[31] A.S.K. Hashmi, G.J. Hutchings, Angewandte Chemie-International Edition 45 (2006) 7896.
[32] S.A.K. Hashmi, Chemical Reviews 107 (2007) 3180.
[33] W.L. Barnes, A. Dereux, T.W. Ebbesen, Nature 424 (2003) 824.
[34] V. Biju, T. Itoh, A. Anas, A. Sujith, M. Ishikawa, Analytical and Bioanalytical Chemistry 391 (2008) 2469.
[35] L. Brus, Accounts of Chemical Research 41 (2008) 1742.
[36] A. Moores, F. Goettmann, New Journal of Chemistry 30 (2006) 1121.
[37] D. Cahen, G. Hodes, M. Grätzel, J.F. Guillemoles, I. Riess, Journal of Physical Chemistry B 104 (2000) 2053.
[38] M. Gratzel, Journal of Photochemistry and Photobiology C 4 (2003) 145.
[39] A. Hagfeldt, M. Gratzel, Chemical Reviews 95 (1995) 49.
[40] P.V. Kamat, Journal of Physical Chemistry B 106 (2002) 7729.
[41] V. Subramanian, E.E. Wolf, P.V. Kamat, Journal of the American Chemical Society 126 (2004) 4943.
[42] A. Wood, M. Giersig, P. Mulvaney, Journal of Physical Chemistry B 105 (2001) 8810.
[43] A. Dawson, P.V. Kamat, Journal of Physical Chemistry B 105 (2001) 960.
[44] P.V. Kamat, Pure and Applied Chemistry 74 (2002) 1693.
[45] C. Aprile, M.A. Herranz, E. Carbonell, H. Garcia, N. Martin, Dalton Transactions (2009) 134.
[46] E. Kowalska, R. Abe, B. Ohtani, Chemical Communications (2009) 241.
[47] J.T. Carneiro, C.C. Yang, J.A. Moma, J.A. Moulijn, G. Mul, Catalysis Letters 129 (2009) 12.
[48] C. Colosio, M. Tiramani, M. Maroni, Neurotoxicology 24 (2003) 577.
[49] E. Evgenidou, K. Fytianos, I. Poulios, Journal of Photochemistry and Photobiology A-Chemistry 175 (2005) 29.
[50] G. Krejcova, K. Kuca, L. Sevelova, Defence Science Journal 55 (2005) 105.
[51] N.J. Simcox, R.A. Fenske, S.A. Wolz, I.C. Lee, D.A. Kalman, Environmental Health Perspectives 103 (1995) 1126.
[52] O. Danek, V. Stengl, S. Bakardjieva, N. Murafa, A. Kalendova, F. Oplustil, Journal of Physics and Chemistry of Solids 68 (2007) 707.
[53] H. Luo, C. Wang, Y. Yan, Chemistry of Materials 15 (2003) 3841.
[54] S.J. Gregg, K.S.W. Sing, Adsorption, Surface area and Porosity, Academic Press, London, 1982.
[55] M. Gratzel, Heterogeneous Photochemical Electron Transfer, CRC Press, Baton Rouge, LA, 1988.
[56] G. Burgeth, H. Kisch, Coordination Chemistry Reviews 230 (2002) 40.
[57] J. Tauc, R. Grigorovici, A. Vancu, Physica Status Solidi 15 (1966) 627.
[58] P. Falcaro, D. Grosso, H. Amenitsch, P. Innocenzi, Journal of Physical Chemistry B 108 (2004) 10942.
[59] P. Innocenzi, P. Falcaro, J.M. Bertolo, A. Bearzotti, H. Amenitsch, Journal of Non-Crystalline Solids 351 (2005) 1980.
[60] M. Mesa, L. Sierra, J. Patarin, J.L. Guth, Solid State Sciences 7 (2005) 990.
[61] H. Zhang, J.F. Banfield, Journal of Materials Chemistry 8 (1998) 2073.
[62] H.X. Li, J.X. Li, Y.N. Huo, Journal of Physical Chemistry B 110 (2006) 1559.
[63] M.Y. Mihaylov, J.C. Fierro-Gonzalez, H. Kno1zinger, B.C. Gates, K.I. Hadjiivanov, Journal of Physical Chemistry B 110 (2006) 7695.
[64] M.M. Alvarez, J.T. Khoury, T.G. Schaaff, M.N. Shafigullin, I. Vezmar, R.L. Whetten, Journal of Physical Chemistry B 101 (1997) 3706.
[65] S. Link, M.A. El-Sayed, Journal of Physical Chemistry B 103 (1999) 8410.
[66] S. Neatu, B. Cojocaru, V.I. Parvulescu, V. Somoghi, M. Alvaro, H. Garcia, Journal of Materials Chemistry 20 (2010) 4050.
[67] G.W. Wagner, P.W. Bartram, O. Koper, J.K. Kenneth, Journal of Physical Chemistry B 103 (1999) 3225.